

# Noncovalent dyads of lanthanide nitride cluster fullerenes $\text{Ln}_3\text{N@C}_{80}$ and bisphthalocyanines $\text{LnPc}_2$ : A DFT Study

Lina M. Bolivar-Pineda<sup>1,2\*</sup>, César Martínez-Flores,<sup>2</sup> Elena V. Basiuk<sup>1</sup>, & Vladimir A. Basiuk<sup>1</sup>.

<sup>1</sup> Instituto de Ciencias Aplicadas y Tecnología, Universidad Nacional Autónoma de México, Circuito Exterior C.U., 04510 Mexico City, Mexico

<sup>2</sup> Instituto de Ciencias Nucleares, Universidad Nacional Autónoma de México, Circuito Exterior C.U., 04510 Mexico City, Mexico

\*linabolivar12@gmail.com

## Background

### Phthalocyanines (Pcs)

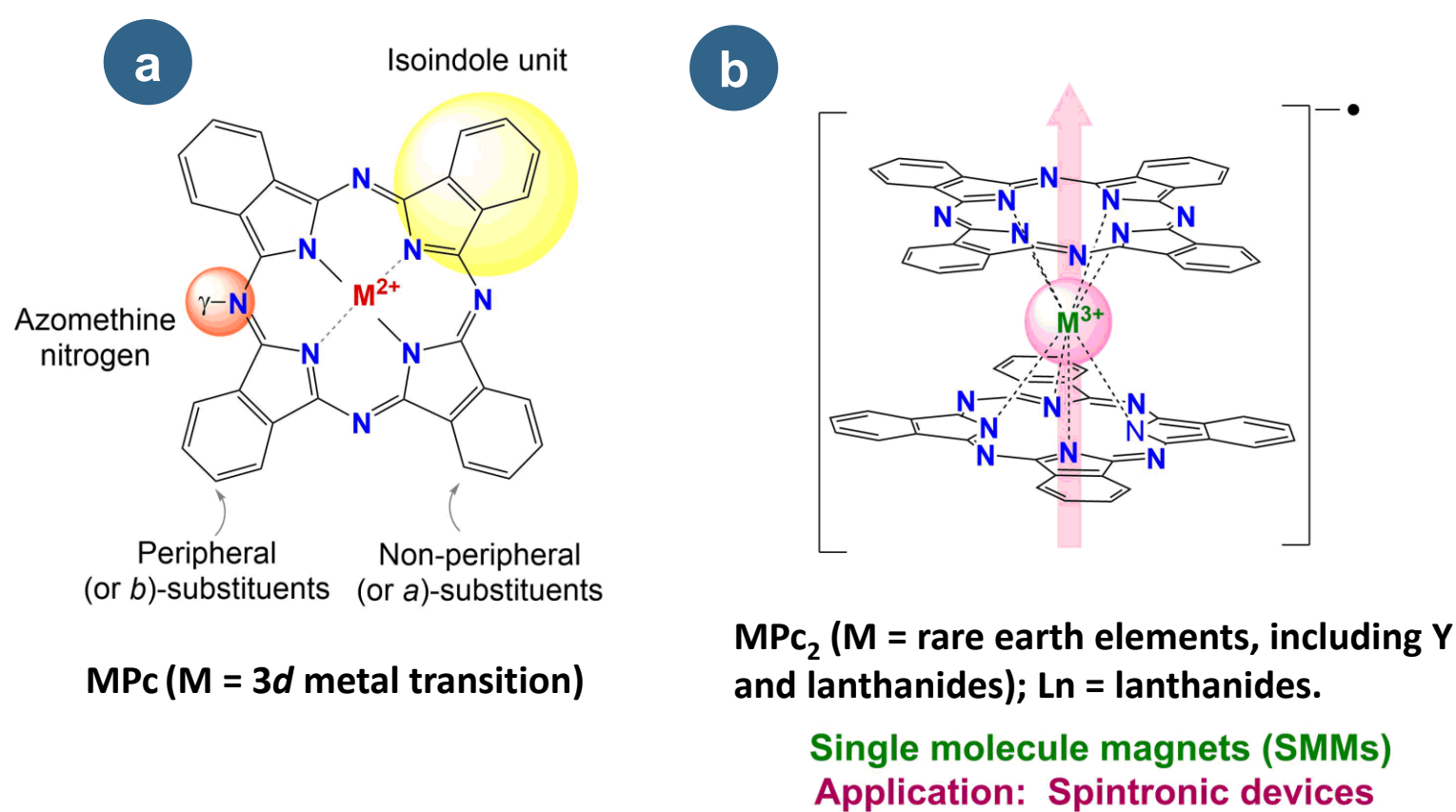


Fig.1. Structure of (a) monophthalocyanines and (b) bisphthalocyanine. [1]

### Carbon nanomaterials + MPC<sub>2</sub>

Noncovalent interactions between  $\text{LnPc}_2$  and carbon nanotubes as well as graphene (with defects), have been investigated using density functional theory (DFT). The most relevant conclusion from the published studies is that the interaction of  $\text{GdPc}_2$  with zigzag CNTs [2] and graphene with 5665 defects [3] leads to changes in spin orientation compared to the isolated components.

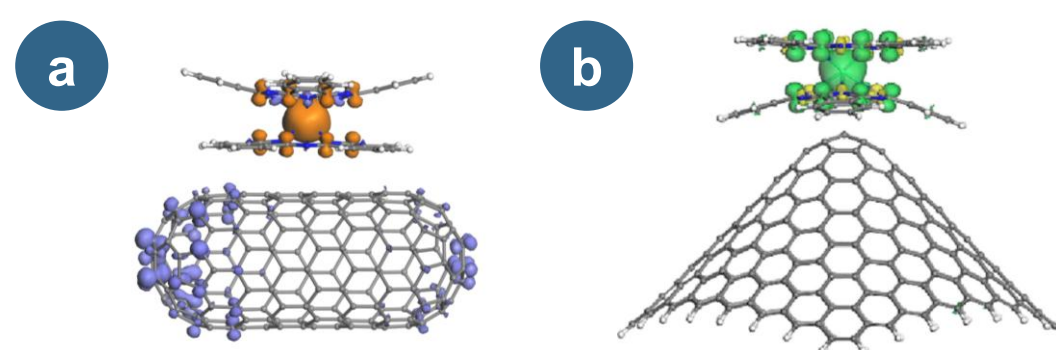


Fig.2. Spin density plots for (a)  $\text{GdPc}_2$ +SWCNTs and (b)  $\text{GdPc}_2$ +G-5665 (Isosurfaces at 0.01 a.u.). [2,3]

a) Violet and orange lobes represent spin-up and spin-down electrons.  
b) Green and yellow lobes represent spin-up and spin-down electrons

### Nitride cluster fullerene ( $\text{Ln}_3\text{N@C}_{80}$ ; NCFs)

What changes occurs in HOMO, LUMO, and spin density distribution of  $\text{LnPc}_2$  (Ln = La, Ce, Gd, Lu) upon interaction with  $\text{Ln}_3\text{N@C}_{80}$ , compared to the isolated  $\text{LnPc}_2$  systems?



### Aim

- To analyze the geometric and electronic property changes of  $\text{LnPc}_2$  upon noncovalent interaction with  $\text{Ln}_3\text{N@C}_{80}$  using DFT.



## Results and discussion

## Computational method

### DFT

**Functional:** general gradient approximation (GGA) functional by Perdew-Burke-Ernzerhof (PBE) in combination with a long-range dispersion correction by Grimme (PBE-D).

**Different basis sets** (DN, DND, DNP) were tested; structures were selected based on agreement with XRD data. DN was used to simulate the dyads.



2

### $\text{LnPc}_2 + \text{La}_3\text{N@C}_{80}$ dyads

#### Structural characteristics

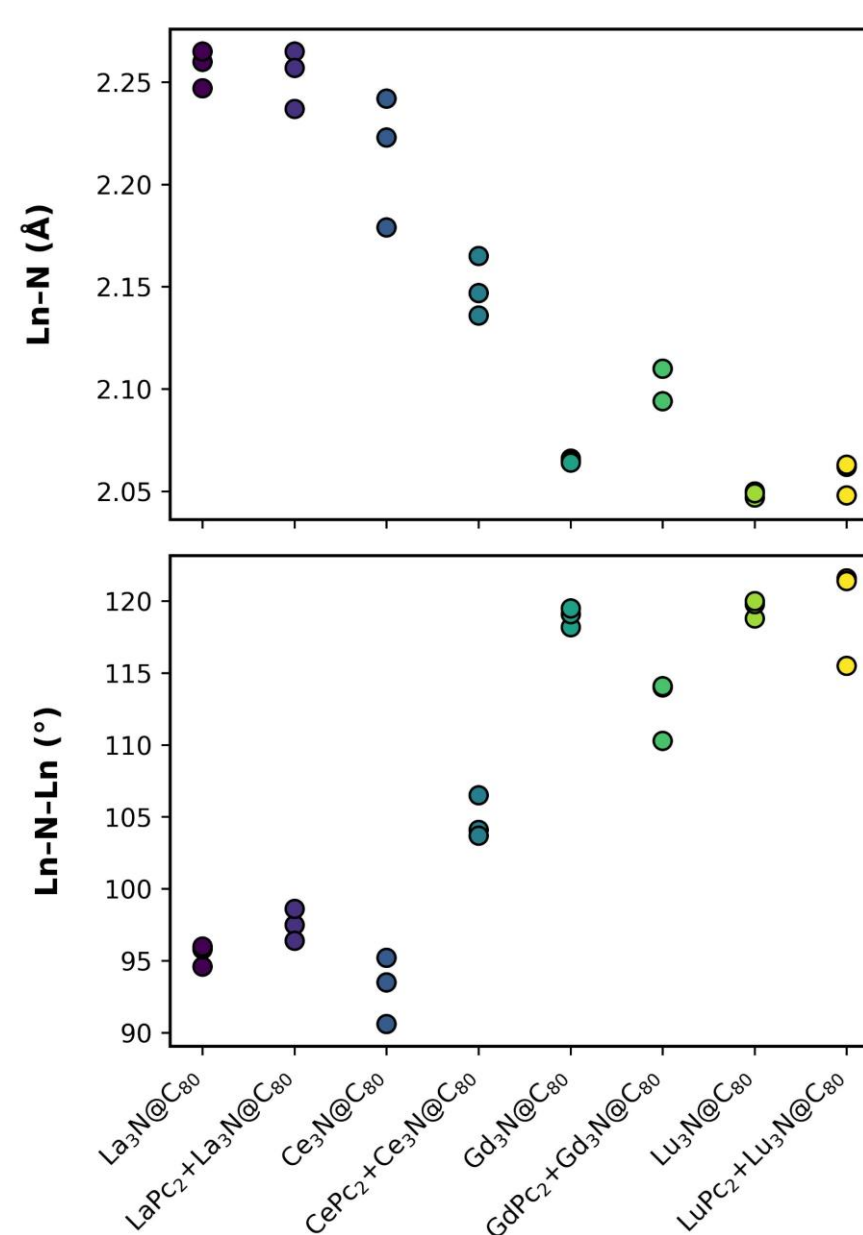


Fig. 4. Comparison of the Ln-N bond lengths (Å; top) and Ln-N-Ln angles (°; bottom) in the isolated lanthanide nitride cluster  $\text{Ln}_3\text{N@C}_{80}$  (Ln = La, Ce, Gd, and Lu) and in the noncovalent  $\text{LnPc}_2 + \text{Ln}_3\text{N@C}_{80}$  dyads.

The changes in spin density distribution are evident in the dyads containing Ce and Gd atoms, contrary to their La and Lu-derived counterparts. The interaction of  $\text{Ce}_3\text{N@C}_{80}$  and  $\text{Gd}_3\text{N@C}_{80}$  with  $\text{CePc}_2$  and  $\text{GdPc}_2$ , respectively, causes redistribution of the spin density, with changes in the orientation of spin-up and spin-down electrons in the encapsulated  $\text{Ce}_3\text{N}$  and  $\text{Gd}_3\text{N}$  clusters.

## Acknowledgements

L. M. B.-P. acknowledges the ELISA ACUÑA Postdoctoral Fellowship Program from the Dirección General de Asuntos del Personal Académico (DGAPA) at the National Autonomous University of Mexico (UNAM). Financial support from UNAM (grant DGAPA-IG100125) is greatly appreciated.

## References

- [1] V.E. Pushkarev, L.G. Tomilova, V.N. Nemykin, Coord. Chem. Rev. 319 (2016). 110–179.
- [2] L.M. Bolivar-Pineda, C. Uriel-Mendoza & V.A. Basiuk. J. Mol. Model. 29. 158 (2023)
- [3] C. Uriel-Mendoza, L.M. Bolivar-Pineda J.R. Mascarós & V.A. Basiuk. Comput. Theor. Chem. 1225. (2023). 114152

#### Electronic properties

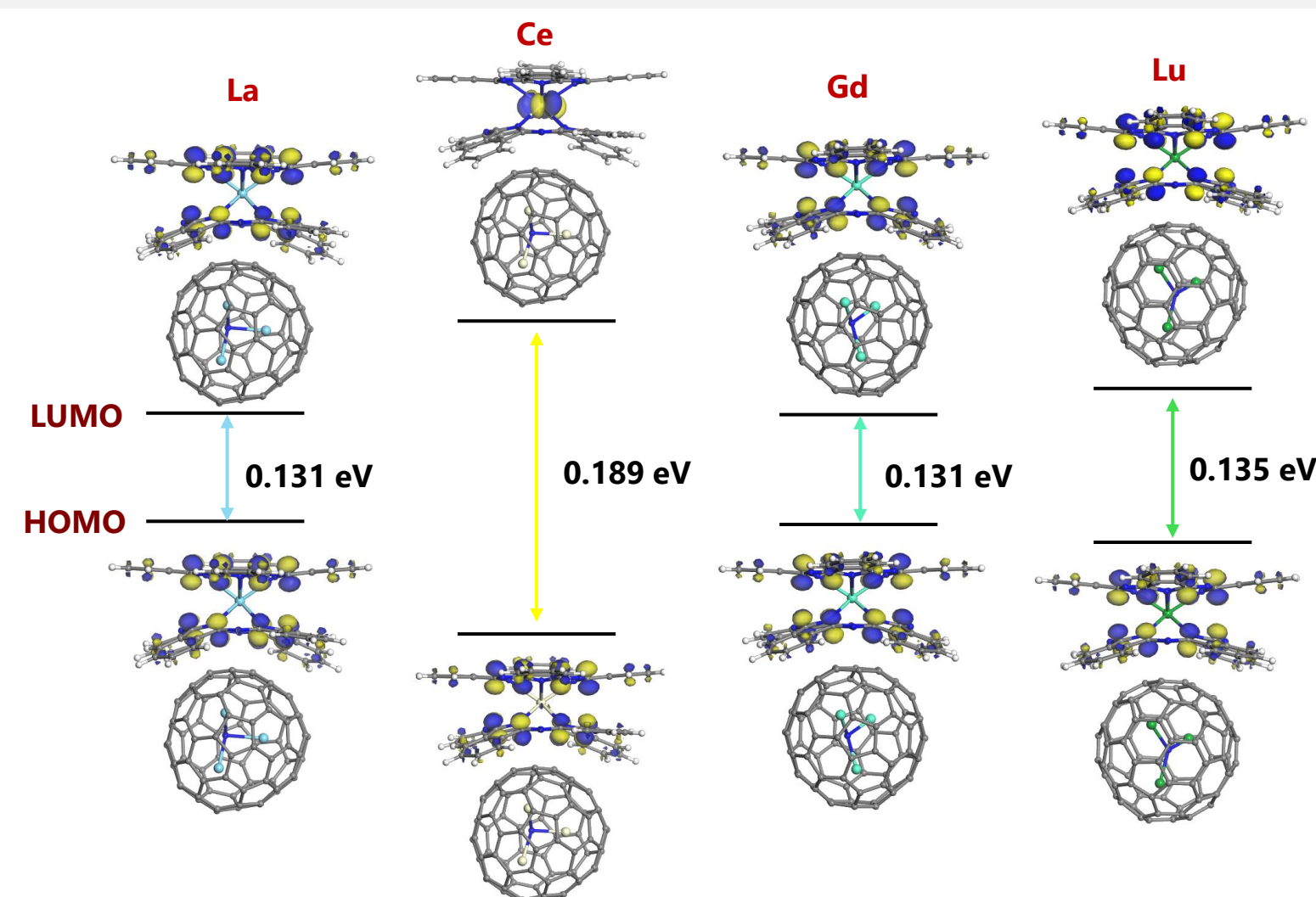


Fig. 5 HOMO and LUMO (isosurfaces at 0.03 a.u.) and gap energies for noncovalent  $\text{LnPc}_2 + \text{Ln}_3\text{N@C}_{80}$  dyads.

#### Spin density

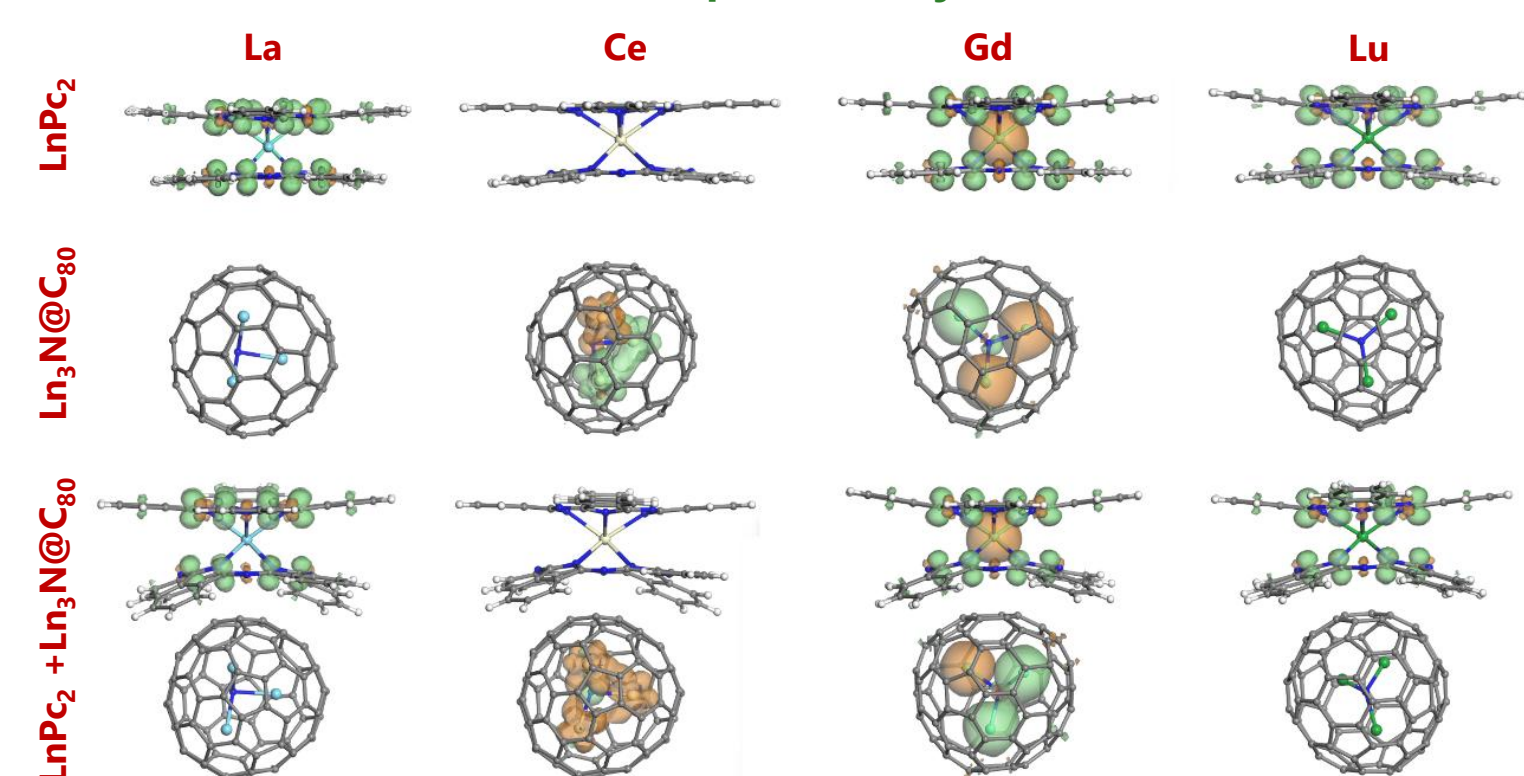


Fig. 6. Comparison of spin density patterns (isosurfaces at 0.01 a. u.) for isolated  $\text{LnPc}_2$  and  $\text{Ln}_3\text{N@C}_{80}$  molecules with those for their noncovalent dyads  $\text{LnPc}_2 + \text{Ln}_3\text{N@C}_{80}$ . The green and orange lobes correspond to spin-up and spin-down electrons, respectively.

## Conclusions

- Using a smaller basis set (DN) proved effective for lanthanide species, with no convergence issue
- Noncovalent  $\text{LnPc}_2 + \text{Ln}_3\text{N@C}_{80}$  interactions induce structural changes in the encapsulated  $\text{Ln}_3\text{N}$  cluster, favoring planar or pyramidal geometries.
- Energy gap values are closer to those of isolated bisphthalocyanines, indicating that the  $\text{LnPc}_2$  component governs the reactivity of the dyad.

## Optimization of isolated bisphthalocyanines and nitride cluster fullerenes

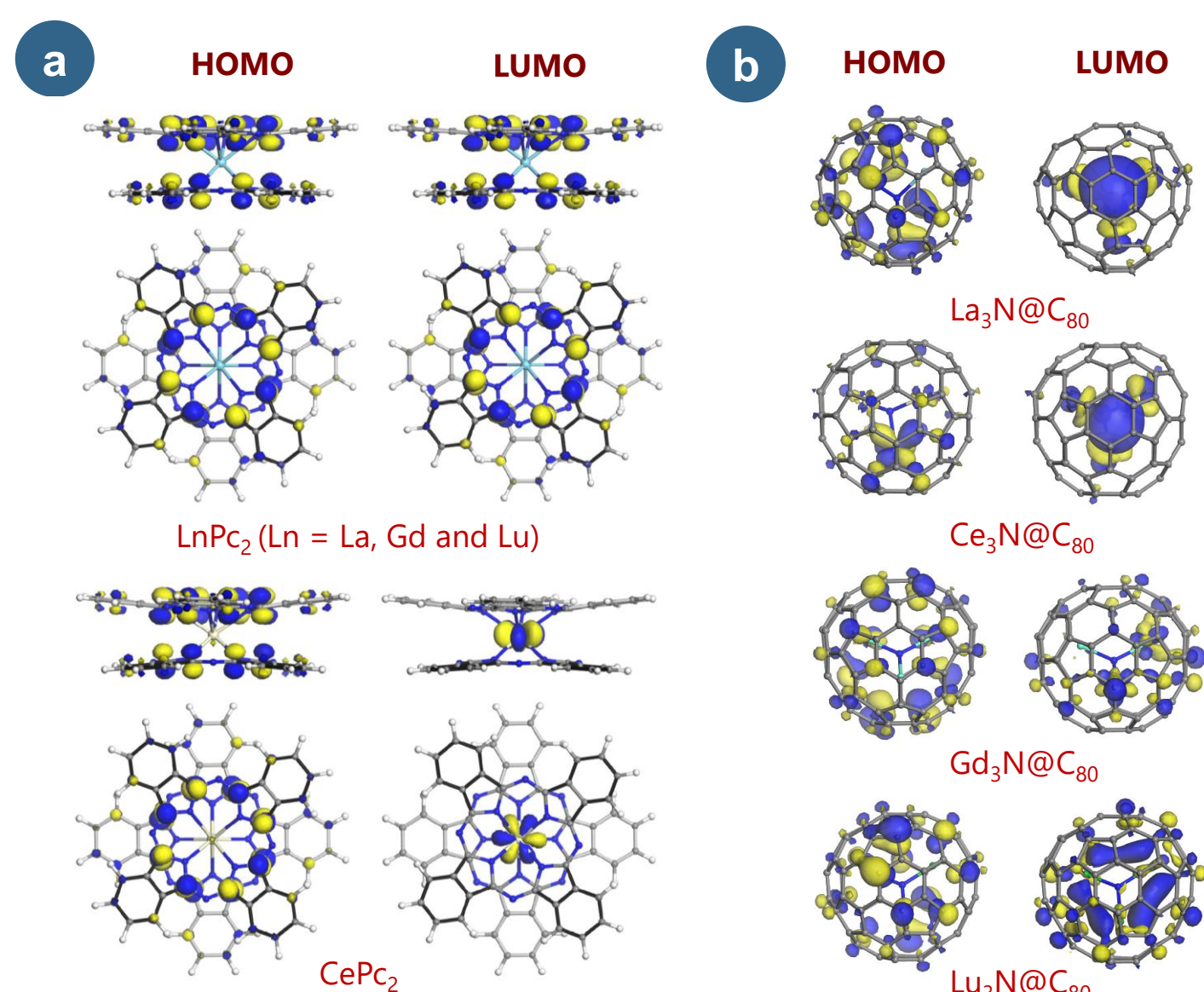


Fig. 3. Frontier orbital distribution (HOMO and LUMO; isosurfaces at 0.03 a.u.) for isolated (a) bisphthalocyanine and (b)  $\text{Ln}_3\text{N@C}_{80}$ .

Table 1. HOMO-LUMO gap energies (in eV) for isolated components  $\text{Ln}_3\text{N@C}_{80}$  and  $\text{LnPc}_2$ .

| System                       | $E_{\text{gap}}$ (eV) |
|------------------------------|-----------------------|
| $\text{La}_3\text{N@C}_{80}$ | 1.371                 |
| $\text{Ce}_3\text{N@C}_{80}$ | 0.862                 |
| $\text{Gd}_3\text{N@C}_{80}$ | 1.457                 |
| $\text{Lu}_3\text{N@C}_{80}$ | 1.528                 |
| $\text{LaPc}_2$              | 0.131                 |
| $\text{CePc}_2$              | 0.196                 |
| $\text{GdPc}_2$              | 0.130                 |
| $\text{LuPc}_2$              | 0.137                 |

